Electronic Supporting Information

Advanced Nanoporous Separators for Stable Lithium Metal Electrodeposition at Ultra-High Current Densities in Liquid Electrolyte

Jingling Yang,[a,b] Chun-Yao Wang,[a,c] Chun-Chieh Wang,[d] Kuei-Hsien Chen,[a,c,e] Chung-Yuan Mou,*[a,f] and Heng-Liang Wu*[a,g]

[a] Center for Condensed Matter Sciences, National Taiwan University, Taipei 10617, Taiwan

[b] School of Environment, Jinan University, Guangzhou 510632, China

[c] Department of Chemistry, National Taiwan Normal University, Taipei 106, Taiwan

[d] National Synchrotron Radiation Research Center, Hsinchu, 30076 Taiwan

[e] Institute of Atomic and Molecular Sciences, Academia Sinica, Taipei 10617, Taiwan

[f] Department of Chemistry, National Taiwan University, Taipei 10617, Taiwan

[g] Center of Atomic Initiative for New Materials, National Taiwan University, Taipei 10617, Taiwan

KEYWORDS: Li metal batteries, Li dendrite, nanoporous separator, mesoporous silica thin film, anodic aluminum oxide

Experimental Section:

Synthesis of MSTF⊥AAO membrane:

Our previous study shows that polystyrene (PS) was spin-coated on the macropores AAO to form a smooth surface layer (PS/AAO), the as-prepared sample was then immersed in an oil-in-water emulsion to grow a single-layer MSTF on the top of PS/AAO membrane. The PS was removed by the calcination. However, the residual PS would block the channels of AAO easily during the spin-coating process. Also, the growth of MSTF on AAO is performed in oil-in-water emulsion under 50 °C for 20 hr (hydrothermal process) which could decrease the mechanical strength of AAO substrate. To solve the problems regarding the residual polymer and the fragile AAO after hydrothermal process, we therefore developed a new method to grow MSTF on AAO substrate in this study.

Polyvinylidene fluoride (PVDF, Kynar 2801) was used as a transfer layer to transfer MSTF on the macropores of anodic aluminium oxide (AAO, pore size of 70 nm, thickness of 56 μm Shengzheng Topmembrane Co. LTD., China) membrane for subsequent growth of a mesoporous silica thin film (MSTF). First, 10.0 wt% PVDF was dissolved in acetone (Acros organics) and dimethyl formamide (Acros organics) mixed solution (acetone: dimethyl formamide = 3:1 v/v) and ultrasonic at 30°C for 1 h. Then, 600 μL of the mixed PVDF solution was spin-coating at 2000 rpm for 30 s on a 2 × 4 cm^2 glass sheet under ultraviolet (UV) light (Longchin 10 W ultraviolet tube) irradiation. Further solvent was evaporated at 60°C for 1 h. The spin-coating procedure were repeated three times. Subsequently, the MSTF can be synthesized onto PVDF membrane in oil-in-water emulsion. AAO did not participate in the hydrothermal process. To remove the residual organic surfactants, the samples were immersed in a hydrochloric acid/ethanol (5 mg/mL, 50 mL) solution for 12~16 h under constant stirring, followed by the MSTF/PVDF/glass sheet was washed by ethanol. The MSTF/PVDF membrane was peeled off the glass sheet. Then the MSTF/PVDF layer was transferred onto AAO membrane (1.6 cm in diameter). Finally, the synthesized MSTF/PVDF/AAO membrane was calcined in air atmosphere by ramping the temperature from 30°C to 500°C at a rate of 2.5°C/min, which was maintained for 15 min. After removing the PVDF by calcination, a dual-layer MSTF⊥AAO membrane composed of continuous MSTF thin membrane with perpendicular mesochannels on AAO membrane were obtained.

Material Characterizations:

Scanning Electron Microscope (SEM): Top-view and edge-view micrographs

were taken from a field emission SEM (Hitachi S-4800) which operated at accelerating voltages of 5 kV. Before SEM measurements, Li metal was thoroughly rinsed with DOL/DME to remove salt residues. The residual solvent was removed under vacuum for 8 h.

Grazing-Incidence Small-Angle X-ray Scattering (GISAXS): GISAXS was conducted at BL23A station in Taiwan Light Source (TLS), National Synchrotron Radiation Research Center (NSRRC), Taiwan. Detailed information is in supporting information. The incidence X-ray energy of 15 keV (0.83 Å) and the sample-to-detector distance of 2.80 m results in a scattering vector (q) range of 0.01-0.62 $Å^{-1}$ that is equivalent to real space distance of 62.8-1.013 nm. The angle of incidence X-ray beam was 0.1°. The scattering data extraction was taken in an X-ray scattering image analysis package (POLAR) installed in NSRRC.

Transmission X-ray Microscopy (TXM): A Synchrotron-based TXM at BL01B1 beamline of TLS (NSRRC, Taiwan) provides 2D radiography and 3D tomography of specimens with 60-nm spatial resolution using a Fresnel zoneplate objective. After the zoneplate, a Zernike phase ring installed at the back focal plane of the zoneplate for phase contrast imaging, which is especially useful for light element material imaging. In this work, the TXM was used to observe whether the Li dendrite penetrated into the AAO-based materials or not. Before the TXM measurements, cycled AAO-based materials were rinsed in the solvent and dried overnight in an Ar-filled glove box with moisture and oxygen level below 1 ppm. AAO-based materials were then sealed in the plastic bag for the acquisition of 2D X-ray radiographies with the sample rotated stepwise.

Contact angle measurements: Contact angle measurements were performed with a Contact Angle Goniometer (FTA125).

Electrolyte preparation:

The electrolytes were 1 M lithium bis(trifluoromethane sulfonyl)imide (LiTFSI, 99.0%, Acros organics) in 1:1 (v/v) solution of 1,2-dimethoxyethane (DME, anhydrous, 99.5 %, Sigma-Aldrich)/1,3-dioxolane (DOL, anhydrous, Sigma-Aldrich) and 1 M Lithium hexafluorophosphate in 1:1 (v/v) solution of ethylene carbonate (EC, Sigma-Aldrich) and diethyl carbonate (DEC, Sigma-Aldrich). Solvents were distilled and stored with molecular sieves. The LiTFSI salt purchased from Sigma Aldrich was further dried at 120°C under vacuum for 8 hours.

Two-electrode coin cell preparation and electrochemical measurements:

A pair of Li metal anodes (300 μm thick) were used in Li-Li symmetric cells. Li and Cu foil (10 μm thick, UBIQ technology Co., LTD) were used in Li-Cu asymmetric

cells. These cells were fabricated in a CR2023 coin cell with a separator including Celgard 2325 (Celgard LLC., USA), AAO, and MSTF⊥AAO, respectively. Cycling processes were carried out by using an Arbin Battery Tester (Model BT 2043, Arbin Instruments Corp., USA) with various current densities ranging from 0.1 mA cm^{-2} to 20 mA cm^{-2}. Each charge and discharge time is set as 30 min.

$LiFePO_4$ (LFP, L＆F Co., Ltd in Korea.)-carbon cathode materials used in Li-LFP batteries were made from a slurry consisting of 80 wt% LFP, 10 wt% carbon black (Super-P Li, Timcal Inc.), and 10 wt% polyvinylidene fluoride (PVDF, Kynar 2801) binder mixed with anhydrous N-methyl-2-pyrrolidone (NMP, Sigma-Aldrich) and stirred overnight. The LFP loading was 5~6 mg/cm^2. The area of electrode is 1.13 cm^2. Li metal is against to MSTF side of MSTF⊥AAO separator. The Li- LFP cells were cycled at a 0.5 C rate (1C=170 mA g^{-1}) at room temperature. The battery performance was conducted at various C rates of 0.1 C, 0.25 C, 0.5 C, 1 C, 2 C, and then 0.1 C between 3.0 and 4.3 V. All the cells were assembled in an Ar-filled glove box with moisture and oxygen level below 1 ppm. Electrochemical impedance spectroscopy (EIS) measurements were conducted at open circuit potential (OCP) after 0th , 4th, 50th, 150th and 200th cycle using an frequency analyzer (Solartron 1255, AMETEK) in a frequency range from 0.01 Hz to 1 MHz with an amplitude of 10 mV and a potentiostat (Solartron 1287, AMETEK).

Demonstration of the advantages of straight channels in MSTF:

The simple theoretical analysis with Peers equation is used to study the limiting flux (J).

First, we give a derivation of the Peers Equation of the highest possible steady state limiting current. At steady state, the limiting electric flux in electrode (J_{lim}) would be balanced by the sum of ion mobility term ($J_{lim}(t_+)$) and diffusional electric flux term ($J_{diffusion}$):

$$J_{lim} = J_{lim}(t_+) + J_{diffusion} \qquad (1)$$

At limiting steady state, the concentration of Li^+ at anode falls to zero. For diffusion one dimensional channel along x-direction, the concentration profile would simply be

$C(x) = (x/L)C_0$ (e.g. $C(0)=0$ and $C(L)=C_0$)

(C_0 is the bulk electrolyte concentration, L is the distance from anode surface)

And for 1-dimensional diffusion, the diffusional current flux would be

$$J_{diffusion} = Q\, D_{app}\, (dC/dx) = Z_c F\, D_{app}\, C_0\, (L)^{-1} \qquad (2)$$

(Q is the molar charge quantity of cation, Z_c=1 is the charge number of the lithium cation, C_0 is the bulk electrolyte concentration, F is the Faraday constant, D_{app} is the apparent diffusion coefficient of lithium cations in the separator membrane, L is the thickness of separator)

Substituting (2) to (1), we get

$J_{lim} = J_{lim}(t_+) + Z_cC_0FD_{app}(L)^{-1}$

$J_{lim}(1- t_+)= Z_cC_0FD_{app}(L)^{-1}$

Since t_+ (transference number of cations) + t_- (transference number of anions) = 1, we get

$$J_{lim} = Z_cC_0FD_{app}/ \{(t-)(L)\} \qquad (3)$$

For a porous and tortuous solid, the apparent diffusion constant is given by

$$D_{app}= \Phi (D_{solution})/\tau$$

($D_{solution}$ is the diffusion coefficient of solution, τ is the tortuosity of the diffusion path, Φ is the volume fraction of void) The simplest mathematical method to estimate tortuosity is the arc-chord ratio: τ=S/*l* (S is the length of the curve, *l* is the distance between two ends) Thus. τ =1 for straight channels and $\tau=\infty$ for a circle.
For our MSTF/AAO materials, the channels are straight and we get τ =1.
For Celgard 2325 separator materials, it has been measured by 3-D electron tomograph (τ =2.2-2.6)

Then we get,

$$J_{lim}= Z_cC_0F\ \Phi\ (D_{solution})\ (\tau)^{-1}\ (L)^{-1}(t_-)^{-1} \qquad (4)$$

In the comparison of Celgard 2325 and MSTF⊥AAO separator, with similar thickness and void fraction, the tortuosity factor (τ) in MSTF⊥AAO and Celgard 2325 indicates that MSTF⊥AAO could tolerate ~ 2.5 times higher limiting current density than Celgard 2325. ($C_{0=}$1M and Zc=1) Also, As the MSTF materials being highly negative charged and immobile, the larger value of t_{Li+} can be obtained. MSTF⊥AAO separator with the larger value of t_{Li+} (smaller value of t_{Li-}) shows higher J_{lim}. This analysis provides physical understanding of the advantages of straight channels in MSTF.

Results and Discussions:

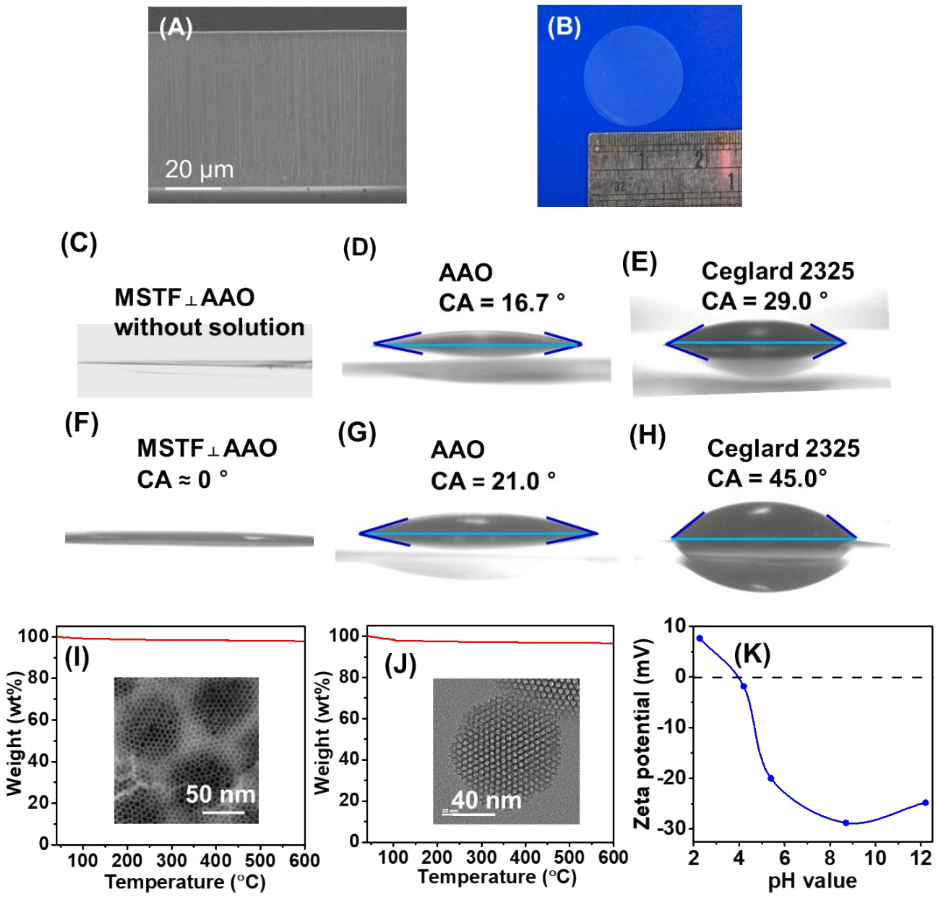

Fig.S1 (A) Cross-section SEM image of MSTF⊥AAO, (B) photograph of MSTF⊥AAO film. Contact angle image of (C) MSTF⊥AAO film without solution, (D) AAO and (E) Celgard 2325 in a solution of 1M LiTFSI DOL/DME. Contact angle image of (F) MSTF⊥AAO film, (G) AAO, and (H) Celgard 2325 in a solution of 1M $LiPF_6$ EC/DEC. Thermal gravity analysis of (I) pristine MSTF⊥AAO membrane and (J) concomitant ex-MSN (SEM image of MSTF⊥AAO and TEM image of ex-MSN after TGA measurements are inset). (K) Zeta potential measurements of MSTF⊥AAO separator.

Thermal gravity analysis of pristine MSTF⊥AAO membrane was conducted to study the thermal stability of MSTF⊥AAO. We found that ~2.2 wt% weight decreases in the initial 200 °C, which attributes to the desorption of surface-adsorbed water. The weight of MSTF⊥AAO kept constant as temperature raises from 200 °C to 600 °C. This

analysis indicates the excellent thermal stability of MSTF⊥AAO.

Table S1. Electrochemical performance of the Li||Li cells with MSTF⊥AAO separator compared with available data in the literature.

Method	Current (mA cm^{-2})	Capacity (mAh cm^{-2})	Time (hour)	Ref.
MSTF⊥AAO separator 1M LiTFSI (DOL/DME=1:1)	0.5	0.25	2000	This work
	2	1	2000	
	3	1.5	2000	
	10	5	1600	
	20	10	400	
MSTF⊥AAO separator 1 M $LiPF_6$ (EC:DEC=1:1)	2	1	2000	
	5	2.5	1600	
20 nm pore-size Al_2O_3 separator 1M LiTFSI (DOL/DME=1:1)	1	1	1560	Ref. (18)
	1.5	1.5	1560	
	3	3	1560	
	10	1	75	
Bacterial cellulose supported poly(methyl vinyl ether-alt-maleic anhydride) as polymer electrolyte	9.5	9.5	250	Ref. (19)
$LiNO_3$-protected, 1 M $LiPF_6$ (EC:DEC)	1	1	1420	Ref. (20)
	2	1	930	
	2	2	690	
	2	5	530	
	5	5	423	
	5	10	290	
	5	20	180	
1 M LiPF6 (EC:DEC) with 0.5 wt% LiF additive	1	4	1700	Ref. (21)
	2	4	580	
	4	4	140	
Lithium in 3D nickel foam host, 1 M $LiPF_6$ (EC:DEC:EMC=1:1:1)	1	1	210	Ref. (22)
	3	1	70	
	5	1	40	

Al-doped $Li_{6.75}La_3Zr_{1.75}Ta_{0.25}O_{12}$ (LLZTO) coated polypropylene (PP) separators 1M LiTFSI (DOL/DME=1:1)	1	1	75	Ref. (23)
LLZTO coated PP separators 1 M $LiPF_6$ (EC/DEC=1:1)	1	1	800	
Carbon nanotubes (CNT) with ZnO layer on Li foil 0.6 M LiTFSI (DOL/DME=1:1) with the addition of 0.4 M $LiNO_3$	1	1	1040	Ref. (24)
	5	1	84	
Dry N2 -passivated Li metal anodes, 1 M $LiPF_6$ (EC:DEC)	1	1	333	Ref. (25)
Poly(ethyl α -cyanoacrylate) based artificial SEI on Li metal, 1 M $LiPF_6$ (EC:DEC)	1	1	400	Ref. (26)

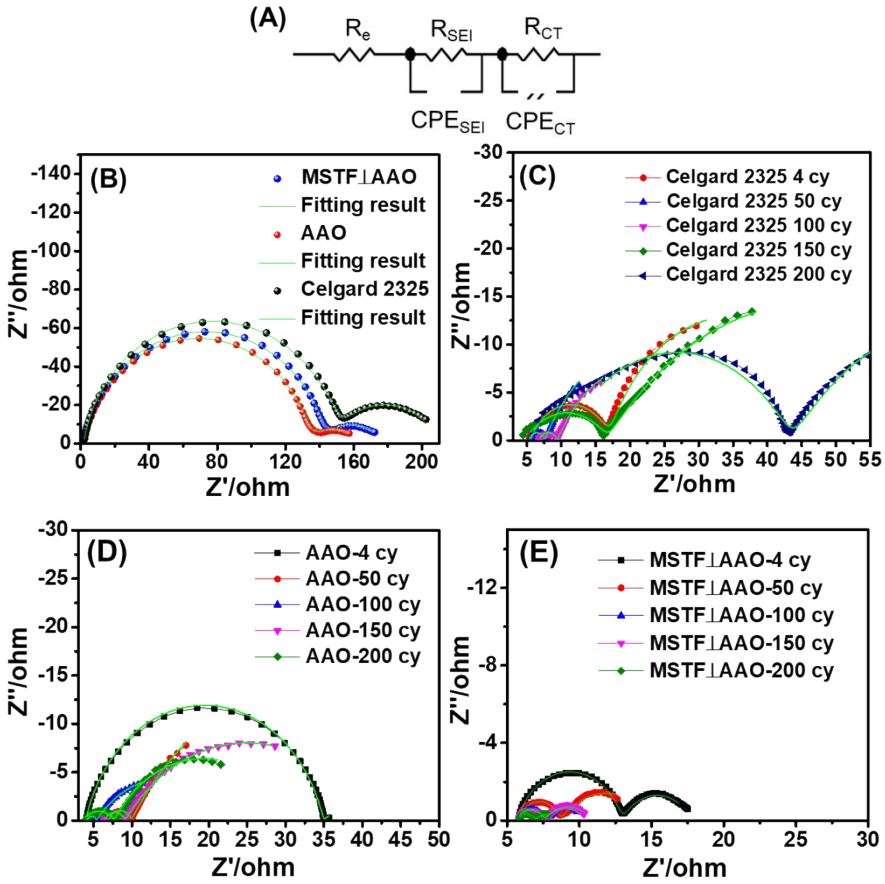

Fig. S2 (A) Equivalent circuit model for fitting impedance spectra. Re is attributed to the bulk resistor and R_{SEI} is the interfacial resistor, CPE_{SEI} and CPE_{CT} are constant phase elements. Nyquist plots of Li-Li symmetric cells with Celgard 2325, bare AAO and MSTF⊥AAO as separator before cycling (B), and with (C) Celgard 2325, (D) bare AAO and (E) MSTF⊥AAO as separator cycled at a fixed current density of 2 mA cm^{-2} and capacity of 1 mAh cm^{-2}, respectively. The electrolyte is 1M LiTFSI in a 1:1 (v/v) solution of DOL/DME.

Aiming at characterizing the interfacial stability in Li metal batteries with different separators, EIS measurements were performed on the identical Li-Li symmetric cells with different separators freshly assembled and after cycles, respectively. Supplementary Fig.S2 shows Nyquist plots of Li-Li symmetric cells with Celgard 2325, bare AAO and MSTF ⊥AAO separator before and after cycling. Fig. 2F shows interfacial resistance of Li metal in Li-Li symmetric cells obtained from impedance

spectra after cycling. The results were fitted by the equivalent circuit model depicted in supplementary Fig. S2A. The resistances obtained from cells with different separators decrease at the beginning of cycling, which are attributed to the formation of the SEI film. After 50 cycles, the cells with AAO and MSTF⊥AAO separators exhibit less variation of interfacial impedance (R_{SEI}), indicating more stable SEI layers are formed with AAO and MSTF⊥AAO separator compared with that of the cells with Celgard 2325 separator. The changes in interfacial impedance can also be correlated with the cycling performance shown in Fig. 2B.

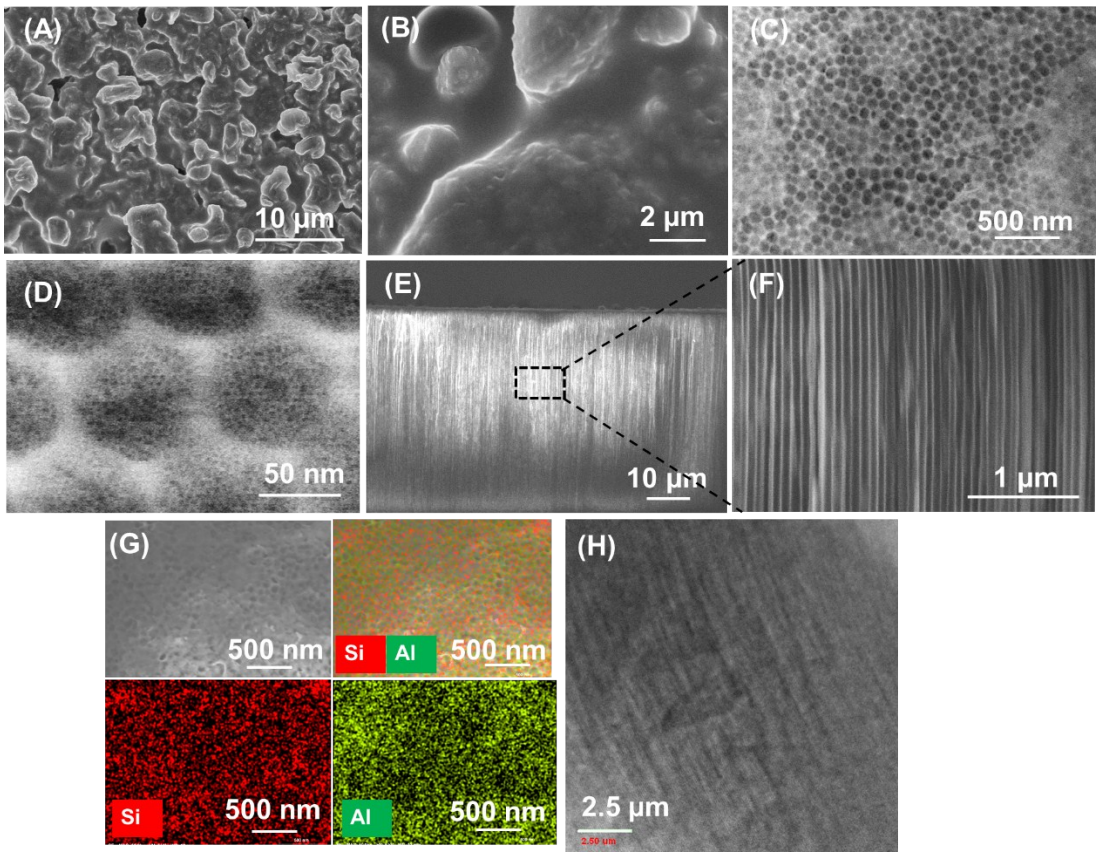

Fig. S3 Surface SEM image of Li metal cycled with (A) AAO side and (B) MSTF side of MSTF⊥AAO separator in a Li-Li symmetric cell at a fixed current density of 2 mA cm^{-2} and capacity of 1 mAh cm^{-2} after 400 repeated Li plating-stripping cycles. The Li metal was stopped at the end of the stripping process. SEM images of the surface of (C-D) MSTF ⊥ AAO separator after 400 cycles. (E-F) Cross-section SEM images of MSTF⊥AAO separator and (G) Si and Al elemental distributions in the surface of MSTF ⊥ AAO separator after cycling. (H) TXM images of MSTF ⊥AAO separator before cycling. The electrolyte is 1M LiTFSI in a 1:1 (v/v) solution of DOL/DME.

Movie S1

Video of AAO separator cycled at a fixed current density of 2 mA cm^{-2} and capacity of 1 mAh cm^{-2} after 400 repeated Li plating-stripping cycles observed from different viewing angles using TXM.

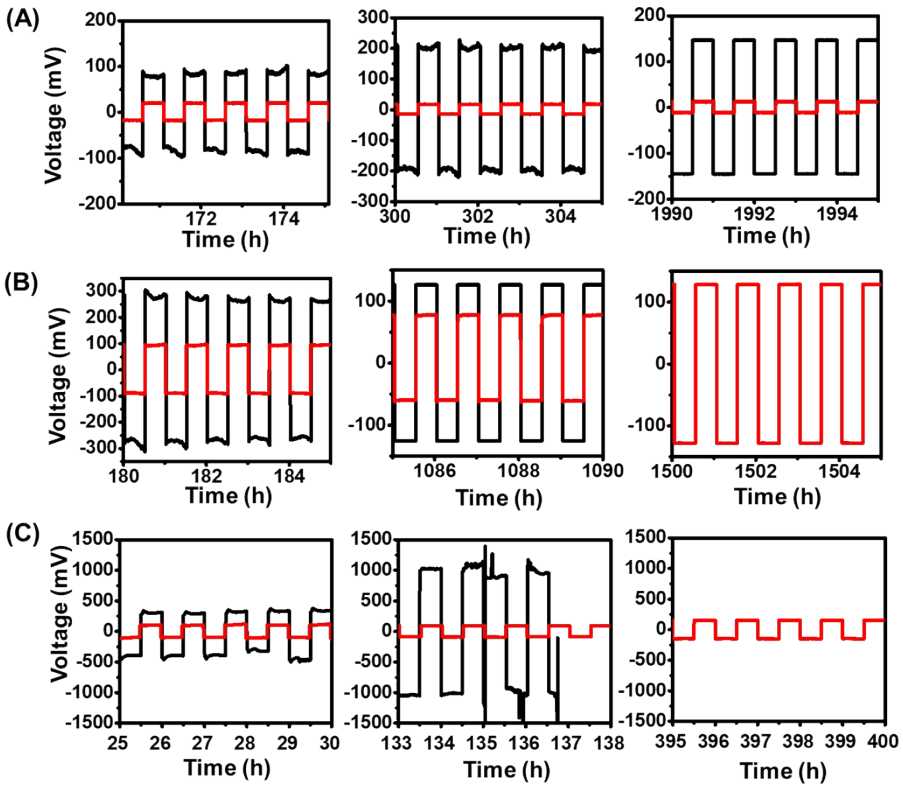

Fig. S4. Galvanostatic cycling profile of Li-Li symmetric cell with AAO (black) and MSTF ⊥ AAO (red) separator at a fixed current density of (A) 3 mA cm^{-2} , (B) 10 mA cm^{-2} and (C) 20 mA cm^{-2}. Each charge and discharge time is set as 30min, respectively. The electrolyte is 1M LiTFSI in a 1:1 (v/v) solution of DOL/DME.

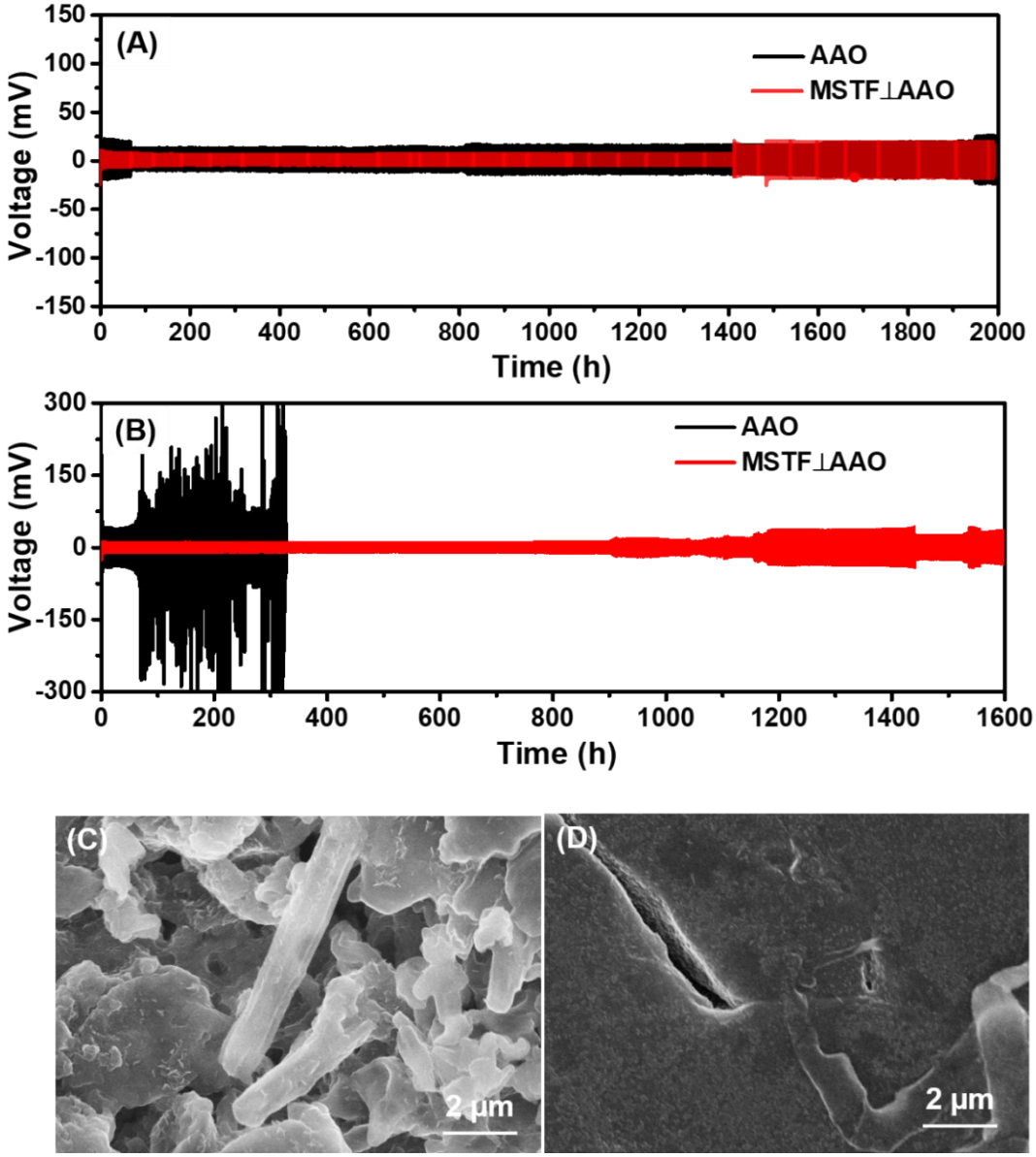

Fig. S5. Galvanostatic cycling performance of Li-Li symmetric cells cycled separator at a fixed current density of (A) 2 mA cm^{-2}, and (B) 5 mA cm^{-2} in 1M $LiPF_6$ with EC/DEC. Each charge and discharge time is 30 min. SEM images of Li metal cycled with (C) AAO side and (D) MSTF side of MSTF⊥AAO separator in a Li-Li symmetric cell at a fixed current density of 10 mA cm^{-2} and capacity of 5 mAh cm^{-2} after 100 repeated Li plating-stripping cycles. Li metal contact with MSTF side was stopped at the end of stripping process. The electrolyte is 1M LiTFSI in a 1:1 (v/v) solution of DOL/DME.

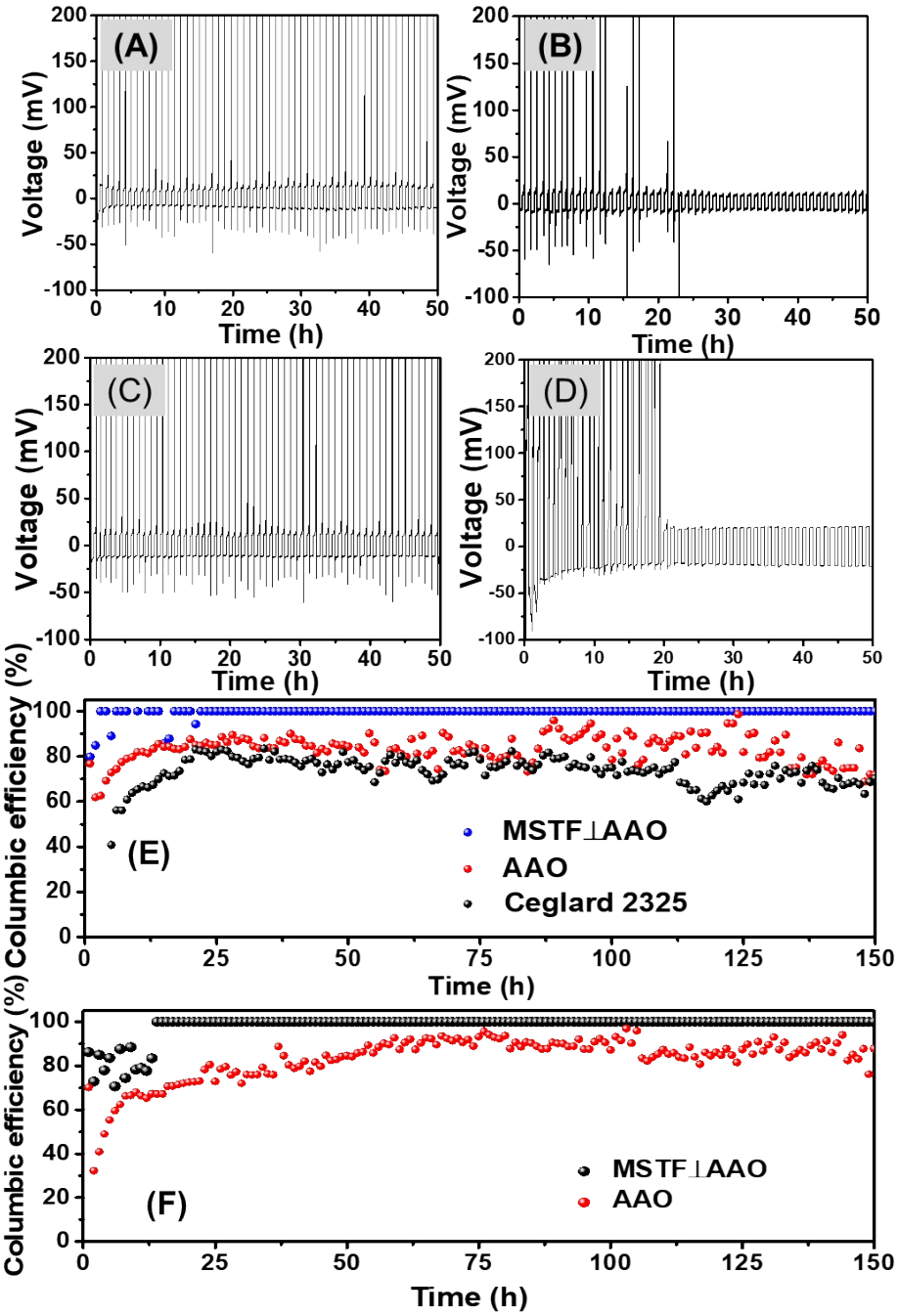

Fig.S6 Galvanostatic cycling performance of Li-Cu asymmetric cell with (A) AAO, and (B) MSTF⊥AAO cycled at a fixed current density of 0.5 mA cm^{-2} and capacity of 0.25 mAh cm^{-2}, (C) AAO and (D) MSTF⊥AAO cycled at a fixed current density of 2 mA cm^{-2} and capacity of 1 mAh cm^{-2}. The electrolyte is 1M LiTFSI in a 1:1 (v/v) solution of DOL/DME. Coulombic efficiency of cell with bare AAO and MSTF⊥AAO cycled at a fixed current density of (E) 0.5 mA cm^{-2} and capacity of 0.25 mAh cm^{-2}, (F) 2 mA cm^{-2} and capacity of 1 mAh cm^{-2}. Cu is against MSTF side in cells with MSTF⊥AAO separators.

Table S2. Coulombic efficiency of Li||Cu cells with MSTF⊥AAO as separator compared with other state of art modifications in the literature.

Method	Current ($mA\ cm^{-2}$)	Capacity ($mAh\ cm^{-2}$)	Cycles	CE	Ref.
MSTF⊥AAO separator 1M LiTFSI (DOL/DME=1:1)	0.5	0.25	150	99.9%	This work
	2	1	150	99.9%	
polyacrylamide-grafted graphene oxide nanosheets@PP separator 1M LiTFSI (DOL/DME=1:1) with 1 wt% $LiNO_3$.	0.5	1	150	98%	Ref. (34)
	1	1	150	98%	
Quaternized polyethylene terephthalate (q-PET) nonwoven fabric 1M LiTFSI (DOL/DME=1:1) with 1 wt % $LiNO_3$ additive.	1	1	100	98%	Ref. (45)
poly-melamine-formaldehyde (PMF)/Li composite anode 1M LiTFSI (DOL/DME=1:1) with 2% $LiNO_3$	1	1	100	98.4%	Ref. (44)
β-phase poly(vinylidene difluoride) (β-PVDF) coated Cu foil 1M LiTFSI (DOL/DME=1:1) with 3 wt% $LiNO_3$ additive	1	2	250	98.7%	Ref. (35)
Thin layer of Silly Putty 1M LiTFSI (DOL/DME=1:1) with 1 wt% $LiNO_3$ additive	1	1	120	97%	Ref. (36)
Poly(dimethylsiloxane) thin film 1M LiTFSI (DOL/DME=1:1) with 1 wt% $LiNO_3$ additive	1	1	100	93.2%	Ref. (42)
Lithium in 3D nickel foam host (1 M $LiPF_6$, EC:DEC:EMC=1:1:1)	1	1	100	86%	Ref. (22)
SiO_2@PMMA core@shell nanospheres on Cu foil, 1 M	1	2	50	90%	Ref. (37)
	0.5	2	50	83%	

$LiPF_6$ (EC:DMC)					
Polyimide coating layer with vertical nanoscale channels, 1 M $LiPF_6$ (EC:DEC)	1	1	40	89%	Ref. (38)
Cu_3N and styrene butadiene rubber (1 M LiPF6 EC/DEC with 10 wt% FEC additive)	1	1	100	97%	Ref. (39)
	0.25	0.5	150	98%	
Hollow Silica Microspheres /carbon nanotubes coated on Cu foil 1M LiTFSI (DOL/DME=1:1)	0.5	2	200	99%	Ref. (40)
carbon nanofibers (CFs) embedded with Au nanoparticles coated on Li 1M LiTFSI (DOL/DME=1:1) with 1 wt% $LiNO_3$.	1	2	400	99.2%	Ref. (45)
Coating Li metal surface with a polymer layer, 1M $LiPF_6$ (EC:EMC:FEC=3:7:1)	0.5	1	200	98%	Ref. (41)

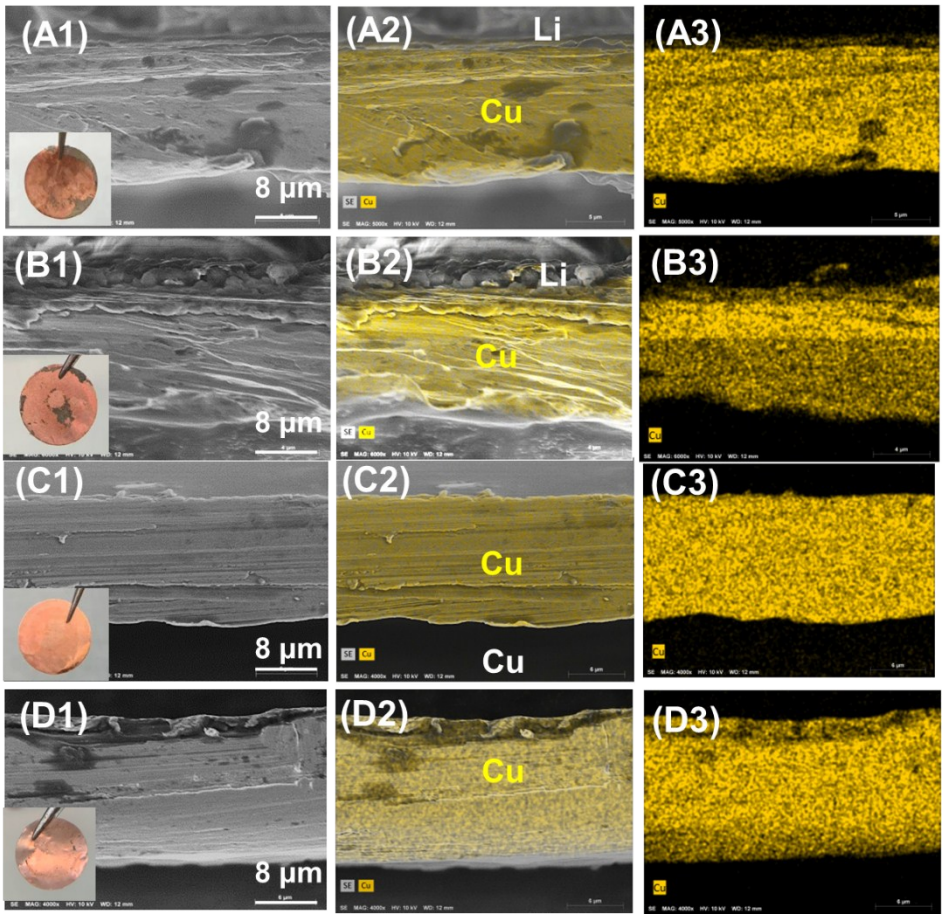

Fig.S7. SEM images, photographs and corresponding Cu element mapping of Cu foil cycled in Li-Cu asymmetric cell with AAO after (A) 50 cycles and (B) 150 cycles at end of stripping process, and with MSTF⊥AAO separator after (C) 50 cycles and (D) 150 cycles at end of stripping process, respectively. Cu is against MSTF side in cells with MSTF⊥AAO separators. The current density is 2 mA cm^{-2} and capacity is 1 mAh cm^{-2}. The electrolyte is 1M LiTFSI in a 1:1 (v/v) solution of DOL/DME.

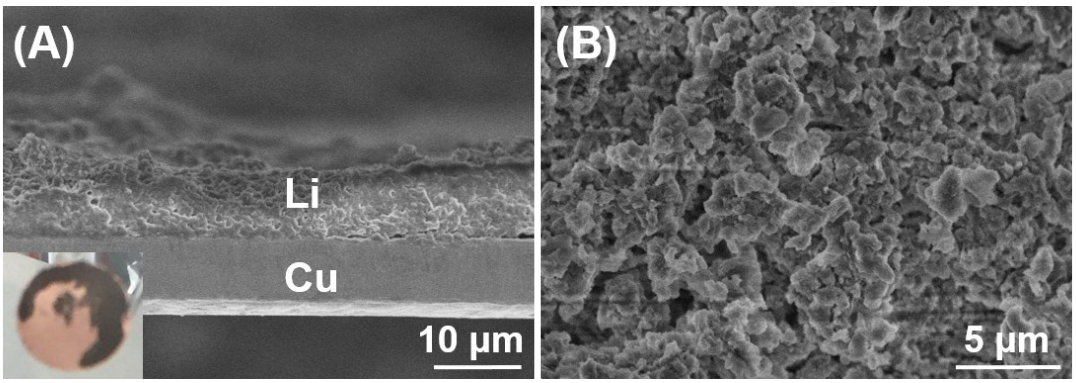

Fig.S8. SEM images, and photographs of Cu foil cycled in Li-Cu asymmetric cell with Celgard 2325 after 150 cycles. The current density is 0.5 mA cm^{-2} and capacity of 0.25 mAh cm^{-2}.

Fig.S7 shows that the surface and cross section SEM images of Cu electrode cycled in Li-Cu asymmetric cells with AAO and MSTF⊥AAO separator after 50 cycles and 150 cycles under a current density of 2 mA cm^{-2} and a capacity of 1 mAh cm^{-2}, respectively. Cu cycled in cells was stopped at the end of stripping process before the SEM measurements. As revealed by the SEM images, elemental mapping and photographs of Cu electrode (Fig. S7A, B), obvious dendritic structure can be observed on the Cu electrode surface cycled with AAO separator, suggesting that residual Li metal (dead Li) occurs on the Cu surface. In contrast, the Cu surface cycled with MSTF⊥AAO separator shows a clean and smooth Cu surface (Fig. S7C, D) which is consistent with excellent CE of Li-Cu cells shown in the present study

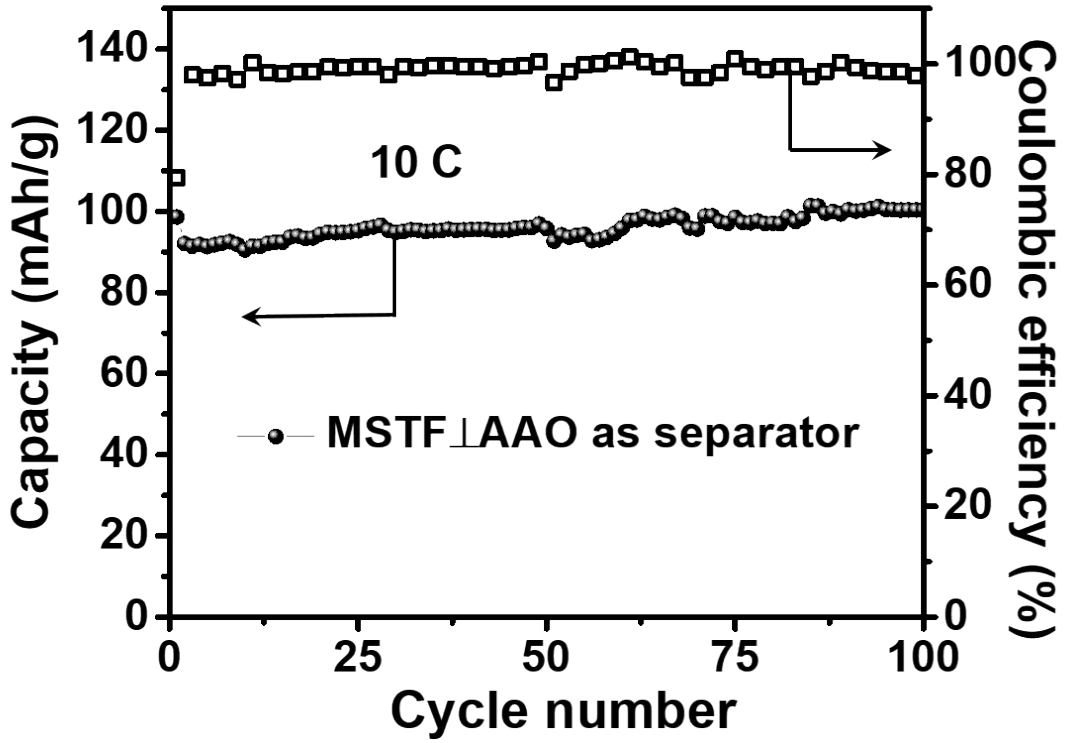

Fig.S9. Cycling performance of Li/$LiFePO_4$ battery with MSTF⊥AAO separator under a current density of 10 C. The electrolyte is 1M LiTFSI in a 1:1 (v/v) solution of DOL/DME.